Analysis and Practical Comparison of Wireless LAN and Ultra-Wideband Technologies for Advanced Localization

Stefan Galler, Jens Schroeder, Golaleh Rahmatollahi, Kyandoghere Kyamakya, and Klaus Jobmann

Abstract—In this paper we compare the capabilities of Wireless LAN and Ultra-Wideband to enable advanced localization systems. The two technologies are compared regarding their suitability towards time-delay-estimation by theoretical bounds as well as by means of practical time-of-flight range estimation in LOS and NLOS conditions in an industrial environment.

Index Terms—**Ultra-Wideband, UWB, Wireless LAN, WLAN, localization, positioning, TDOA**

I. INTRODUCTION

Indoor localization has become an important field of research with its potential for applications in private and industrial environments. Especially for production, logistics, factory and building automation or security and safety applications, combined indoor communication and localization systems with sub-meter accuracy are regarded as a key enabling technology to a whole variety of new services.

Two technologies seem to be appropriate candidates to fulfill the desired functionality: Wireless LAN (IEEE 802.11) because of its high market penetration for communications and also increasingly for localization based on received signal strength methods, offering accuracies of some meters, and Ultra Wideband (UWB), which is just starting for high-rate, short-range multimedia transfer, but research and standardization activities target lower-rate and longer-range concepts, because of its promising precise localization.

To achieve robust and reliable sub-meter accuracy localization in challenging areas as industrial environments, advanced localization techniques have to be applied. Time-of-flight measurements instead of received signal strength methods, in combination with advanced filtering and tracking,

relying on precise time delay estimates as well as the capability to resolve multipath components and the ability to distinguish between line-of-sight (LOS) and non-line-of-sight (NLOS) conditions are regarded as essential for such systems. The goal of this paper is hence to practically compare the capabilities of the two technologies by means of time-of-flight range estimation in LOS and NLOS conditions in an industrial environment.

The paper is organized as follows. Section II compares range estimation minimum variances capabilities using the Cramer-Rao Lower Bound. In Section III, the measurement system setup and the signal processing applied are described. Section IV presents the measurement campaign and respective results. The paper finalizes with a conclusion in Section V.

II. RANGE ESTIMATION BOUNDARIES

The accuracy of time-of-flight based localization depends on the geometrical constellation of sources and receivers and on the accuracy of the range estimates. In this paper we concentrate on the latter. The Cramer-Rao lower bound is widely used as a lower bound for an unbiased estimator. In the case of an all-white-Gaussian-noise channel, the variance $\sigma_{\hat{\tau}}^2$ of the time delay estimate is bounded by [1]

$$\sigma_{\hat{\tau}}^2 \geq \frac{1}{8\pi^2 \beta_f^2 SNR},\tag{1}$$

where *SNR* represents the signal to noise ratio available at the receiver and β_f is the effective bandwidth of the received signal defined by

$$\beta_f \triangleq \left[\int_{-\infty}^{\infty} f^2 \left| S(f) \right|^2 df \Big/ \int_{-\infty}^{\infty} \left| S(f) \right|^2 df \right],\tag{2}$$

and $S(f)$ is the Fourier transform of the signal. As it can be observed, the impact of the effective bandwidth β_f is quadratic, compared to the available *SNR*, which is linear. The effect on time delay estimation using the correlation method can be seen in Fig. 1. The normalized autocorrelation peak of an Ultra-Wideband signal having 1.7 GHz of bandwidth is depicted in the top figure, the normalized autocorrelation peak

S. Galler, J. Schroeder, G. Rahmatollahi and K. Jobmann are with the Institute of Communications Engineering (IKT, University of Hannover, Hannover, Germany (phone: +49 511 762-2814; fax: +49 511 762-3030; e-mail: (galler, jens.schroeder, gola, jo)@ant.uni-hannover.de).

K. Kyamakya is with the Institute of Informatics Systems, University of Klagenfurt, Klagenfurt, Austria (phone: +43 463 2700-3540, fax: +43 463 2700-3598, e-mail: kyamakya@isys.uni-klu.ac.at).

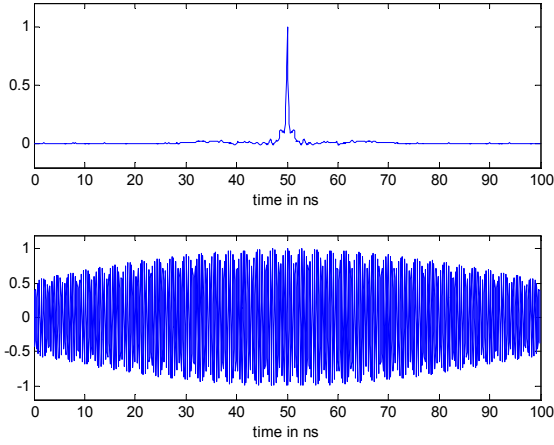of an IEEE 802.11b Wireless LAN having 22 MHz in the bottom.

Fig. 1. Normalized autocorrelation peak of Ultra-Wideband (1.7 GHz) and Wireless LAN (22 MHz) signals.

The much narrower peak of the Ultra-Wideband autocorrelation as a result of the larger bandwidth, allows more precise time delay estimates, especially in the case of multipath conditions, were multiple copies of the autocorrelation function form an additive overlay.

III. MEASUREMENT SYSTEM SETUP

This sections describes the setup of the measurement system, the applied signal processing, the metrics used to compare the measurements and the test of system functionality.

A. General System Setup

The general setup of the measurement system is the same for both technologies, Ultra-Wideband and Wireless LAN. Central component of the measurement system is a high-speed digital sampling oscilloscope, which in conjunction with a PC running Matlab operates as a fully digital receiver at Nyquist rate (see Fig. 2).
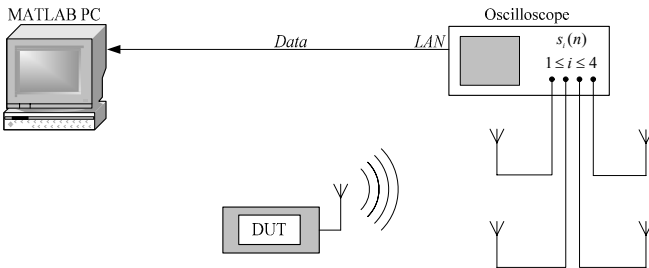

Fig. 2. General Measurement System Setup.

As sampling oscilloscope, we use an Agilent infinium 54855A, running at a sample rate of F_S=10 GS/s with a memory depth of 262.144 samples per channel. When triggered, the oscilloscope simultaneously captures signals received by the four antennas connected to its inputs. For signal processing, all recorded data is subsequently transferred to a standard PC running Matlab. Commercially available Arc Freedom antennas are used, which feature acceptable pulse as well as continuous wave radiation and reception characteristics in the utilized frequency range [2].

The Ultra-Wideband test device is based on a simple mono-phase pulser circuit described in [3]. The design has been extended to be capable of using the avalanche effect of two transistors, resulting in a bi-phase pulse generator. Pulse-durations are in the order of sub-nanoseconds, corresponding to a measured bandwidth of approximately 1.7 GHz. Assuming a fully balanced system, pulse peak power according to pulse peak amplitude of 7.3 V can be estimated to be 30 dBm into a 50 Ω load. Average pulse power at pulse repetition frequency 3.2 MHz can be estimated to be 0 dBm into a 50 Ω load. As measurement signal, we use a 32 chip bi-phase modulated PRN pulse-train. Because of the bandpass characteristics of the antennas, only the frequency range from 0.7 to 1.7 GHz was used, resulting in an effective bandwidth of 1 GHz. A more detailed description of the Ultra-Wideband test device can be found in [4].

The Wireless LAN test device is a standard off-the-shelve IEEE 802.11b D-Link DI-541 access point router, configured to operate on channel 1 (2.412 MHz). Because of its good auto-correlation properties, we use the IEEE 802.11b physical layer convergence protocol (PLCP) preamble as measurement signal [5].

B. Signal Processing

To calculate the time delay estimates, all measurement data are transferred from the oscilloscope to the PC. Fig. 3 shows the direct cross-correlation receiver structure implemented in Matlab, considering as example channel 1 and channel 2:
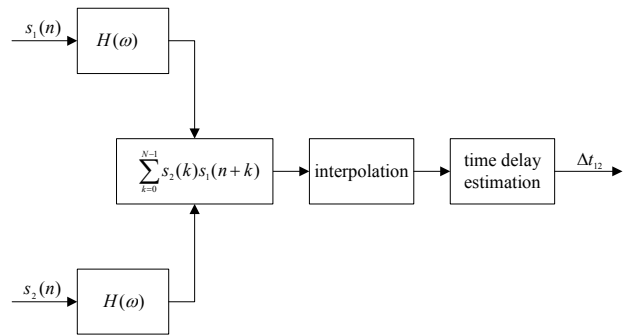

Fig. 3. Direct cross-correlation receiver implementation in Matlab.

Before cross-correlation, each channel $s_i(n), 1 \leq i \leq 4$ is pre-filtered with $H(\omega)$ to suppress out of band interference. In the case of Ultra-Wideband, $H(\omega)$ is implemented as a bandpass filter with passband frequencies from 0.7 to 1.7 GHz. In the case of Wireless LAN, $H(\omega)$ is implemented as a bandpass filter with 22 MHz bandwidth at center frequency 2.412 MHz.

The time delay differences Δt_{12}, Δt_{13}, Δt_{14}, Δt_{23}, Δt_{24} and Δt_{34} are estimated by a maximum search of the cross-correlation function

$$\Delta t_{ij} = t_i - t_j = \arg\max_\tau \int_{-T/2}^{T/2} s_j(t)s_i(t+\tau)dt, \qquad (3)$$

where t_i and t_j denote the absolute times of arrival at antenna i and j, respectively, and

$$1 \le i < j \le N. \qquad (4)$$

N represents the total number of antennas. The TDOA estimates Δt_{ij} are converted to range differences Δd_{ij} through multiplication by the speed of light c:

$$\Delta d_{ij} = c\Delta t_{ij} = c(t_i - t_j) = d_i - d_j. \qquad (5)$$

As in our case cross-correlation is performed in the digital discrete-time domain, the time delay estimation resolution is limited to the duration of the sample period. In order to further increase the resolution, interpolation algorithms can be applied, as the exact time delay estimate is determined by the maximum of the corresponding continuous-time correlation function, instead of the discrete-time sequence.

Especially for quasi sinusoidal continuous wave signals, as the Wireless LAN signal, interpolation prior to maximum detection is essential, as because of sampling, the discrete-time maximum does not necessarily correspond to the equivalent continuous-time maximum [6].
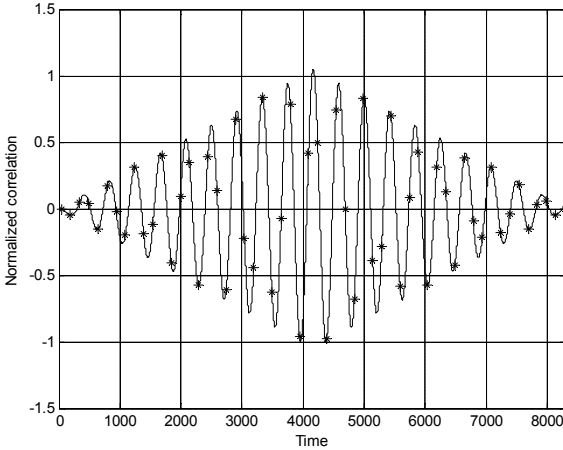

Fig. 4. Correlation peak of a quasi sinusoidal signal sampled slightly above Nyquist rate (The continuous line is showing the continuous-time signal and the crosses are showing the discrete-time sampled signal).

As it can be seen in Fig. 4, the maximum search in the discrete-time domain can result in time delay estimation errors of multiple periods of the quasi-sinusoidal signal, even when sampled above Nyquist rate. In order to avoid such errors in the measurement system, the corresponding continuous-time correlation function is further approximated in the digital domain by interpolation through zero padding and subsequent lowpass filtering [7].

C. Error Metrics

The error metrics used throughout this paper to compare measurement results are: the simple error

$$e_l^{<1>} = \left\| \hat{\mathbf{x}}_l - \mathbf{x}_l \right\|, \qquad (6)$$

defined as the Euclidean distance between the real position $\mathbf{x}_l$ and the estimated position $\hat{\mathbf{x}}_l$, the arithmetic mean

$$\mu_e = \frac{1}{P}\sum_{l=1}^{P} e_l^{<1>}, \qquad (7)$$

of P measurements, the root mean square (RMS) error

$$e_{RMS}^{<P>} = \sqrt{\frac{\sum_{l=1}^{P} e_l^{<1>2}}{P}}, \qquad (8)$$

the standard deviation

$$\sigma_e = \sqrt{\frac{1}{P-1}\sum_{l=1}^{P}\left(e_l^{<1>} - \mu_e\right)^2}, \qquad (9)$$

and an estimate of the corresponding cumulative distribution function $cdf(e^{<1>})$.

D. Test of System Functionality

System functionality has been verified in two steps. First, the system was tested fully wired with equal length cables, in order to avoid all antenna and radio channel propagation effects. Fig. 5 exemplarily shows the propagation delay differences estimated for channel 1 and channel 2 using the Wirelss LAN test device.
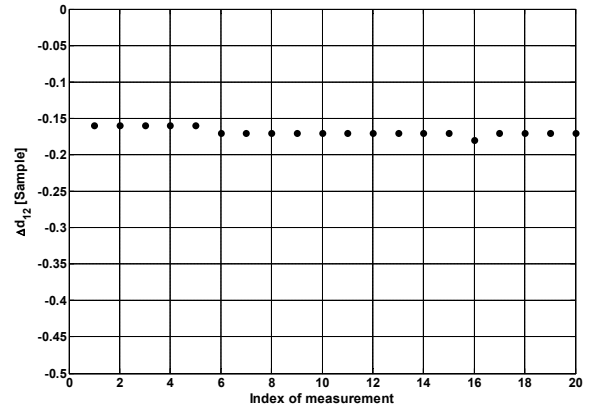

Fig. 5. Wired propagation delay difference estimates using Wireless LAN

The arithmetic mean μ_e of approximately 0.17 Samples (0.5 cm) from expected value zero results from physically not exactly equally long cables. The standard deviation σ_e of 0.005 Samples (0.16 mm) originates from noise in the test signal, timing jitter and analog-to-digital conversion noise of the oscilloscope and can be regarded as the overall measurement system's accuracy.

In a second step, the system was tested in an anechoic chamber, including antenna effects but minimizing radio channel effects. Fig. 6 exemplarily shows the propagation delay differences estimated for channel 1 and channel 2 using the Wirelss LAN test device.
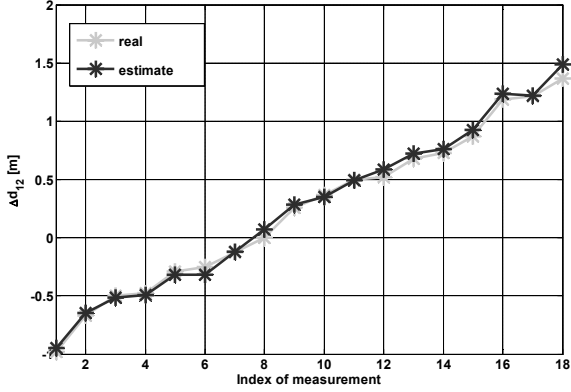

Fig. 6. Anechoic chamber propagation delay difference estimates using Wireless LAN.

The arithmetic mean μ_e of these measurements is 3.8 cm, with a standard deviation σ_e of 3.1 cm. This accuracy is still acceptable, considering antenna effects as well as errors of real position determination, and the system is hence accepted as functional.

IV. MEASUREMENT RESULTS

Real world measurements were conducted in an industrial storage environment, equipped with concrete ceilings, floor, and columns as well as multiple metallic objects (see Fig. 7).

Fig. 7. Photograph of the measurement environment.

Each measurement series was taken moving the transmitting antenna in 10 cm steps along a 9.9 m long straight line, resulting in $N = 100$ measurements (see Fig. 8).
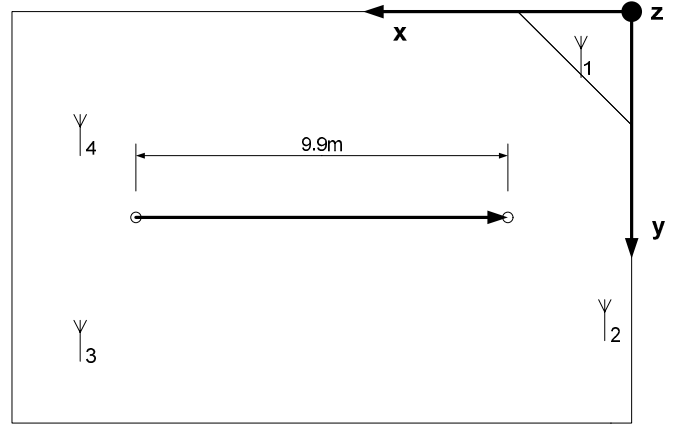

Fig. 8. Measurement setup showing the straight line measured along and the positions of the four receiving antennas.

The four receiving antennas were positioned at locations

$$\begin{bmatrix} x_1 & y_1 & z_1 \\ x_2 & y_2 & z_2 \\ x_3 & y_3 & z_3 \\ x_4 & y_4 & z_4 \end{bmatrix} = \begin{bmatrix} 1.712 & 0.827 & 3.249 \\ 1.373 & 9.520 & 0.880 \\ 19.026 & 10.715 & 3.184 \\ 18.929 & 4.444 & 0.824 \end{bmatrix} m . \qquad (10)$$

All real positions of the mobile device and the infrastructure were determined using a Zeiss Elta C3 total station.

Two measurement series were conducted. The first series consists of time-difference-of-arrival measurements with an always existing LOS component. The second series was taken with the LOS path component explicitly blocked, representing NLOS conditions.

A. Line-of-Sight Measurements

Because of the indoor environment described above, the channels were subject to severe multipath. However, in this measurement series, LOS paths were existent at all positions of the mobile device. Fig. 9 shows the estimated range differences using the Ultra-Wideband pulse generator as mobile device.
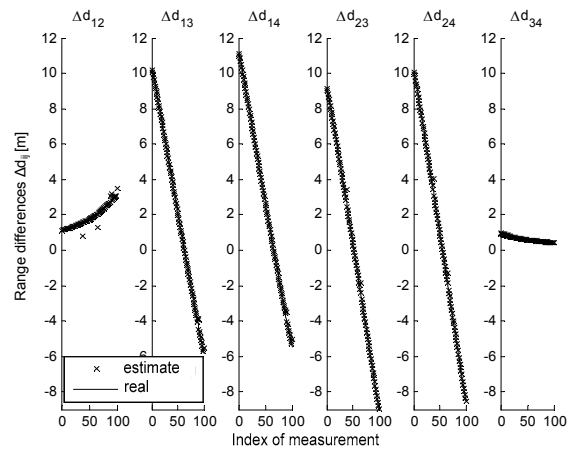

Fig. 9. UWB range differences among all 4 antennas with the straight line showing the real and the crosses showing the estimated range differences.

As it can be observed, estimated values and real values form a good match. The few outliers, which can be found for example in Δd_{12}, could be easily compensated in subsequent localization algorithms. The root mean square error $e_{RMS}^{<P>}$ of theses measurements is 0.096 m with a standard deviation σ_e of 0.086 m. The corresponding estimated cumulative error distribution function $cdf(e^{<1>})$ is depicted in Fig. 10. The relatively few outliers can be recognized here in the flat part of $cdf(e^{<1>})$ for values above 97%.
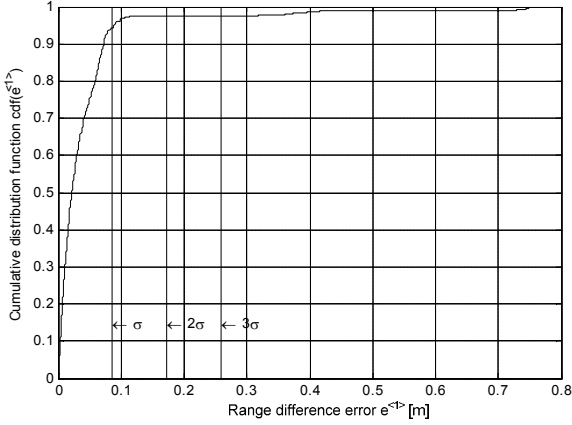
Fig. 10. UWB cumulative distribution function.

Fig. 11 shows the estimated range differences using the same measurement setup as before, but with the Wireless LAN transmitter as mobile device. As it can be observed, the results are much worse. The root means square error $e_{RMS}^{<P>}$ of theses measurements is 10.569 m with a standard deviation σ_e of 7.240 m. The conglomeration of estimates at the top and at the bottom is due to the limitation of estimates to their geometrically maximal possible real values.
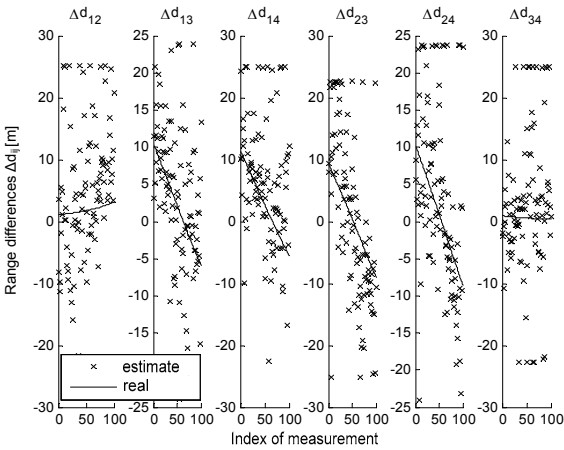
Fig. 11. Wireless LAN range differences among all 4 antennas with the straight line showing the real and the crosses showing the estimated range differences.

The corresponding estimated cumulative error distribution function $cdf(e^{<1>})$ depicted in Fig. 12 also shows the severely lower accuracy compared to Ultra-Wideband.
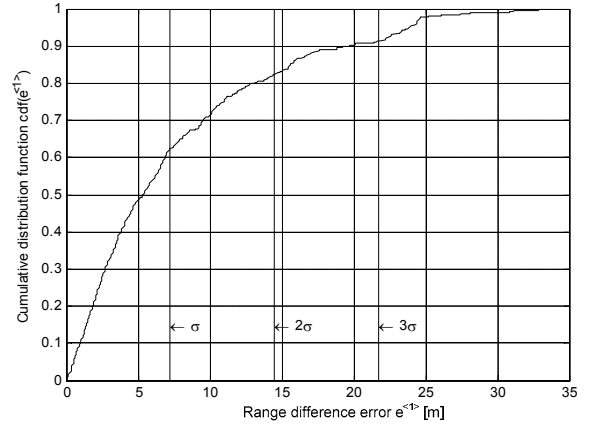
Fig. 12. Wireless LAN cumulative distribution function.

Table I summarizes the performance metrics of the two measurement sets:

TABLE I
ACCURACY PERFORMANCE

Metric	Ultra Wideband	Wireless Lan
$e_{RMS}^{<P>}$	0.096 m	10.596 m
μ	0.042 m	7.742 m
σ	0.086 m	7.240 m

It can be concluded for line-of-sight-conditions in multipath environments, that Ultra-Wideband offers a significantly higher ranging accuracy than Wireless LAN.

B. Non Line of Sight Measurements

For the case of NLOS measurements, the measurement system has been changed. An absorbing wall in front of antenna 2 was used to block the direct path to this antenna at all positions of the mobile device, resulting in NLOS conditions (see Fig. 13).
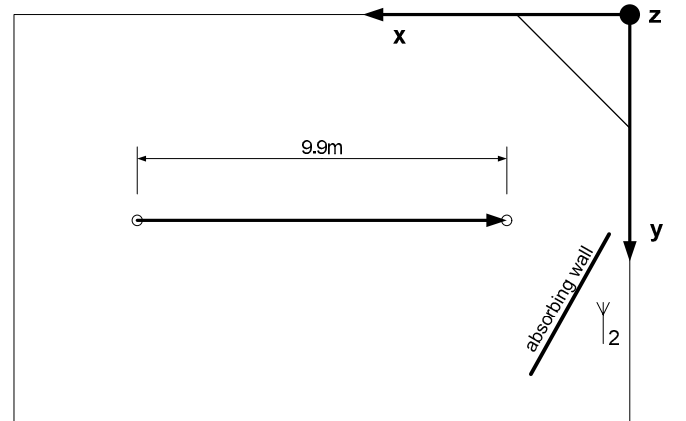
Fig. 13. Measurement setup with absorbing wall in place, for non-line-of-sight measurements.

In order to avoid cross channel effects, resulting from the cross-correlation of two respective wireless channels, a wired template of the transmitted signal was used instead. The

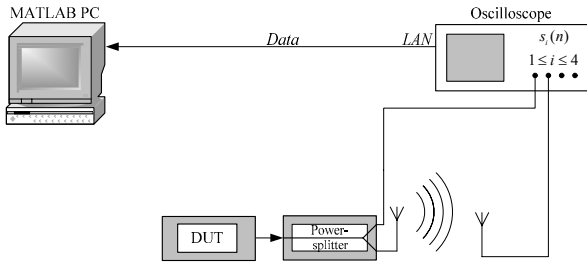template was recorded on channel 1 using a power splitter (see. Fig. 14).

Fig. 14. System setup for Non Line Of Sight measurements.

Two measurement sets were conducted for this scenario: The first set without any blocking object, the second set with the absorber wall in front of antenna 2. The results are depicted in Fig. 15.
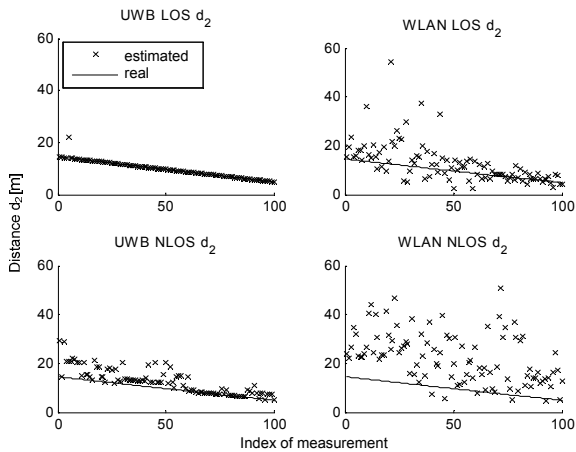

Fig. 15. Comparison of LOS and NLOS time delay estimates.

As it can be observed from Fig. 15, the variation from LOS to NLOS leads to degradation of accuracy for both technologies.
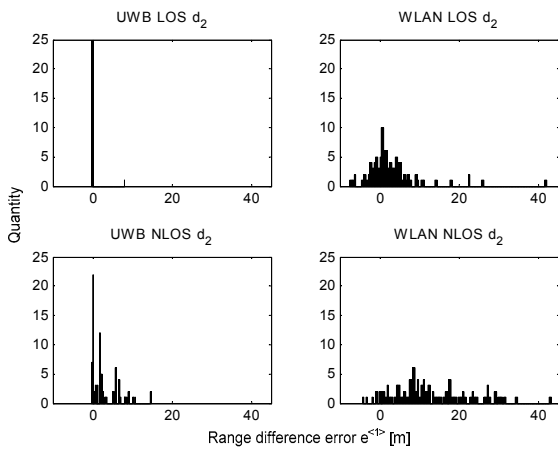

Fig. 16. Histograms of LOS and NLOS distance errors.

But while the error histogram in the case of Wireless LAN simply seems to widen (see Fig. 16), Ultra Wideband allows the detection of dominating paths, resulting in error clusters, which are quasi parallel to the real mobile device distance (see lower left of Fig. 15). The time delay information contained in these quasi parallel error clusters, which are strongly spatially correlated to the direct LOS component, is still valuable for advanced localization and tracking algorithms to gain positioning information.

V. CONCLUSION

Ultra-Wideband signals and IEEE 802.11b Wireless LAN signals have been compared regarding their capabilities for advanced indoor localization. The two technologies were analyzed regarding their suitability towards time-delay-estimation by theoretical bounds as well as by means of practical time-of-flight range estimation in LOS and NLOS conditions in an industrial environment.

As predicted by the theoretical bounds, in LOS conditions, Ultra-Wideband offers a significantly higher ranging accuracy. In NLOS conditions, multipath components, containing information valuable to advanced localization algorithms, can only be resolved using Ultra-Wideband signals.

The significantly better ranging accuracy as well as the superior capabilities in non-line-of-sight conditions demonstrate the much higher potential of Ultra-Wideband compared to Wireless LAN to enable advanced localization systems in indoor environments.

REFERENCES

[1] S. Gezici, T. Zhi, G. B. Giannakis, H. Kobayashi, A. F. Molisch, H. V. Poor, and Z. Sahinoglu, "Localization via ultra-wideband radios: a look at positioning aspects for future sensor networks," *Signal Processing Magazine, IEEE,* vol. 22, pp. 70-84, 2005.
[2] ARC Wireless Solutions Inc., *ARC Freedom Antenna.* Wheat Ridge, Colorado, USA, 2004.
[3] S. P. Lohmeier, R. Rajaraman, and V. C. Ramasami, "Development of an ultra-wideband radar system for vehicle detection at railway crossings," presented at Ultra Wideband Systems and Technologies, 2002. Digest of Papers. 2002 IEEE Conference on, 2002.
[4] J. Schroeder, S. Galler, and K. Kyamakya, "A Low-Cost Experimental Ultra-Wideband Positioning System," presented at IEEE International Conference on Ultra-Wideband, Zurich, 2005.
[5] ANSI/IEEE Std 802.11, "Part 11: Wireless LAN Medium Access Control (MAC) and Physical Layer (PHY) Specifications," 1999 Edition (R2003).
[6] L. Xiaoming and H. Torp, "Interpolation methods for time-delay estimation using cross-correlation method for blood velocity measurement," *Ultrasonics, Ferroelectrics and Frequency Control, IEEE Transactions on,* vol. 46, pp. 277-290, 1999.
[7] I. Cespedes, Y. Huang, J. Ophir, and S. Spratt, "Method for estimation of subsample time delays of digitized echo signals," *Ultrason. Imaging,* vol. 17, pp. 142-171, 1995.